Hui Gu,[1] Jingwen Yu,[1] Daoyin Dong,[1] Qun Zhou,[2] Jian-Ying Wang,[3] Shengyun Fang,[4] and Peixin Yang[1,2]

# High Glucose–Repressed CITED2 Expression Through miR-200b Triggers the Unfolded Protein Response and Endoplasmic Reticulum Stress

*Diabetes 2016;65:149–163 | DOI: 10.2337/db15-0108*

**High glucose in vivo and in vitro induces neural tube defects (NTDs). CITED2 (CBP/p300-interacting transactivator with ED-rich tail 2) is essential for neural tube closure. We explored the regulatory mechanism underlying CITED2 expression and its relationship with miRNA and endoplasmic reticulum (ER) stress. miR-200b levels were increased by maternal diabetes or high glucose in vitro, and this increase was abrogated by transgenic overexpression of superoxide dismutase 1 (SOD1) or an SOD1 mimetic. CITED2 was the target of miR-200b and was downregulated by high glucose. Two miR-200b binding sites in the 3′-untranslated region of the CITED2 mRNA were required for inhibiting CITED2 expression. The miR-200b mimic and a CITED2 knockdown mimicked the stimulative effect of high glucose on unfolded protein response (UPR) and ER stress, whereas the miR-200b inhibitor and CITED2 overexpression abolished high glucose–induced UPR signaling, ER stress, and apoptosis. The ER stress inhibitor, 4-phenylbutyrate, blocked CITED2 knockdown–induced apoptosis. Furthermore, the miR-200b inhibitor reversed high glucose–induced CITED2 downregulation, ER stress, and NTDs in cultured embryos. Thus, we showed a novel function of miR-200b and CITED2 in high glucose–induced UPR and ER stress, suggesting that miR-200b and CITED2 are critical for ER homeostasis and NTD formation in the developing embryo.**

Diabetes induces cell apoptosis, a causal event among many diabetes complications (1–3). Our previous studies have demonstrated that maternal diabetes in pregnancy triggers program cell death in the developing neuroepithelium, which leads to neural tube defects (NTDs) in offspring (3–7). Human studies have shown that as the degree of maternal hyperglycemia increases, so does the incidence of NTDs (8,9). In addition, high glucose directly induces neural stem cell apoptosis and NTD formation in cultured rodent embryos (5,6), supporting the hypothesis that high glucose is a primary causative event in diabetic embryopathy. Although it has been shown that endoplasmic reticulum (ER) stress, gene dysregulation, and caspase activation (10–12) are involved in maternal diabetes in vivo and high glucose in vitro–induced apoptosis (3,13–15), it is unknown whether altered gene expression contributes to unfolded protein response (UPR) and ER stress. It is also unclear how high glucose alters development gene expression that leads to NTD formation.

microRNAs (miRNAs) are small endogenous noncoding RNAs that play important gene-regulatory roles (16–18). miRNAs suppress gene expression by binding to the 3′-untranslated region (3′-UTR) of mRNAs with imperfect complementation, resulting in direct translational repression, mRNA destabilization, or a combination of the two (19). Primary miRNA transcripts are cleaved by the endonuclease Drosha to produce precursor miRs, which are 60- to 70-nt-long imperfect hairpin structures (20). In the cytoplasm, precursor miRNAs are further processed by the endonuclease Dicer, resulting in a mature miRNA, the guide strand for gene regulation, and a passenger strand,

[1]Department of Obstetrics, Gynecology, and Reproductive Sciences, University of Maryland School of Medicine, Baltimore, MD
[2]Department of Biochemistry and Molecular Biology, University of Maryland School of Medicine, Baltimore, MD
[3]Cell Biology Group, Department of Surgery, University of Maryland School of Medicine, Baltimore, MD
[4]Center for Biomedical Engineering and Technology, University of Maryland School of Medicine, Baltimore, MD

Corresponding author: Peixin Yang, pyang@upi.umaryland.edu.

Received 21 January 2015 and accepted 5 October 2015.

This article contains Supplementary Data online at http://diabetes.diabetesjournals.org/lookup/suppl/doi:10.2337/db15-0108/-/DC1.

which is degraded and does not play a role in gene regulation (16). miRNAs exert pleiotropic actions under physiological and pathophysiological conditions (17,21). Differential miRNA expression is observed during embryonic neurulation and in maternal sera of NTD-affected pregnancies (22,23), suggesting a possible role of miRNAs in diabetes-induced NTDs.

ER stress is indispensible for high glucose–induced neural stem cell apoptosis. Misfolded protein accumulation in the ER lumen leads to the activation of the UPR (24–26). The ER transmembrane proteins, IRE1α (inositol-requiring enzyme 1 α) and PERK (protein kinase RNA-like endoplasmic reticulum kinase), act as sensors of UPR signaling (24). Prolonged UPR signaling causes a severe form of ER stress, which induces apoptosis (27). A recent study has demonstrated that decreased miRNA-322 leads to ER stress (28); therefore, it is highly possible that there is a link between miRNAs and ER stress and that both participate in high glucose–induced UPR, ER stress, and apoptosis.

CBP/p300-interacting transactivator with ED-rich tail 2 (CITED2) is a transcription coactivator that is essential for embryogenesis, and its deletion causes NTDs by increasing neural stem cell apoptosis (29,30). However, information related to the regulation of CITED2 expression and its cellular functions is scarce. Because high glucose induces NTDs similar to those seen in *Cited2*$^{-/-}$ embryos (3–5), we hypothesize that altered CITED2 expression mediates the effect of high glucose on UPR activation and ER stress leading to neural stem cell apoptosis.

In the current study, we found that high glucose upregulates miR-200b expression and that elevated miR-200b promotes ER stress and apoptosis through silencing CITED2. It has been demonstrated that CITED2 is required for the survival of neural stem cells of the developing neural tube (29,30). Therefore, we reveal a new miR-200b–CITED2–ER stress circuit that may play a critical role in high glucose–induced cell apoptosis that is the etiology of the initiation of diabetes and a range of diabetes complications.

## RESEARCH DESIGN AND METHODS

### Animals and Regents

Wild-type (WT) C57BL/6J mice were purchased from The Jackson Laboratory (Bar Harbor, ME). Superoxide dismutase 1 (SOD1)-transgenic (Tg) mice in C57BL/6J background were revived from frozen embryos by The Jackson Laboratory (stock no. 002298). Streptozotocin (STZ) from Sigma-Aldrich (St. Louis, MO) was dissolved in sterile 0.1 mol/L citrate buffer (pH 4.5). The SOD1 mimetic tempol was purchased from Alexis Italia (Vinci, Florence, Italy). Sustained-release insulin pellets were purchased from Linshin, Canada. The procedures for animal use were approved by the University of Maryland School of Medicine Institutional Animal Care and Use Committee.

### Mouse Models of Diabetic Embryopathy

Our mouse model of diabetic embryopathy has previously been described (3,5). Briefly, 10-week old WT female mice were injected daily with 75 mg/kg i.v. STZ over 2 days to induce diabetes. Using STZ to induce diabetes is not a complicating factor because STZ is cleared from the bloodstream rapidly (STZ serum half-life, 15 min) (31) and pregnancy is not established until 1–2 weeks after STZ injection (7). Diabetes was defined as a 12-h fasting blood glucose level of ≥14 mmol/L. Insulin pellets were subcutaneously implanted in these diabetic mice to restore euglycemia prior to mating. To generate SOD1 embryos, we crossed SOD1-Tg male mice with nondiabetic or diabetic WT female mice. Male and female mice were paired at 3:00 P.M., and pregnancy was established by the presence of the vaginal plug the next morning, and noon of that day was designated as embryonic day 0.5 (E0.5). On E5.5, insulin pellets were removed to ensure that the developing embryos would be exposed to a hyperglycemic environment during neurulation (E8–E10.5). WT female mice were treated with vehicle injections and sham operations on insulin pellet implantation/removal as nondiabetic controls. On E8.75 (at 6:00 P.M.), mice were euthanized and conceptuses were dissected out of the uteri, and then yolk sacs were removed from the embryos. The embryos were used for analyses.

### Cell Culture, Transfection, and miR-200b Mimic and Inhibitor Treatment

C17.2 mouse neural stem cells, obtained from European Collection of Cell Culture, were maintained in DMEM (5 mmol/L glucose) supplemented with 10% FBS, 100 units/mL penicillin, and 100 μg/mL streptomycin. The C17.2 cells are newborn mouse cerebellar progenitor cells transformed with retroviral v-myc (32). Lipofectamine RNAiMAX (Invitrogen, Grand Island, NY) was used according to the manufacturer's protocol for transfection of small interfering (si)RNA into the cells, using 1% FBS culture conditions. The mirVana miRNA mimic and the miRNA inhibitor of miR-200b, the negative control oligo (cat. no. 4464058) for the miR-200b mimic, and the negative control oligo (cat. no. 4464076) for the miR-200b inhibitor were purchased from Ambion (Austin, TX). The miR-200b inhibitor is a single-stranded RNA-based oligonucleotide that is designed to bind to and inhibit endogenous miR-200b. The biotin-labeled miR-200b and the biotin-labeled negative control (*Caenorhabditis elegans* miR-67) were custom made by Dharmacon (Lafayette, CO). CITED2-siRNA (sc-35960) and control siRNA-A (sc-37007) were obtained from Santa Cruz Biotechnology (Dallas, TX).

### Plasmid Construction

The full-length CITED2 coding region (CR) or its 3′-UTR and different 3′-UTR fragments with or without the predicted miR-200b binding sites were amplified and subcloned into the pmirGLO Dual-Luciferase miRNA Target Expression Vector (Promega, Madison, WI) to generate the pmirGLO-Luc-CITED2-CR and pmirGLO–CITED2–3′-UTR. The

sequence and orientation of the fragments in the luciferase reporters were confirmed by DNA sequencing and enzyme digestions. Luciferase activity was measured using the Dual-Luciferase Assay System (Promega), and the levels of pmirGLO-Luc-CITED2-CR or pmirGLO–Luc–CITED2–3′-UTR luciferase activities were normalized to *Renilla* luciferase activity and were further compared with the levels of luciferase mRNA in every experiment. All primer sequences for generating these constructs are provided in Supplementary Table 1.

### Immunoblotting

Immunoblotting were performed as previously described (3,33). The following primary antibodies were used at dilutions of 1:1,000 to 1:2,000 in 5% nonfat milk: CITED2 (Santa Cruz Biotechnology), CHOP, phospho-(p-)PERK, (p-)IRE1α, (p-)eIF2α (eukaryotic translation initiation factor 2A), and cleaved caspase 3 (Cell Signaling Technology). Signals were detected using the SuperSignal West Femto Maximum Sensitivity Substrate kit (Thermo Scientific). All experiments were repeated in triplicate. Antibody information is listed in Supplementary Table 2.

### miRNA and RNA Extraction and Real-Time PCR

Total RNA was isolated from embryos or cultured cells using the mirVana miRNA isolation kit (Ambion) and reverse transcribed using the NCode VILO miRNA cDNA synthesis kit (Invitrogen). Real-time PCR for CITED2, β-actin, miR-200b, and small nuclear RNA U6 was performed using Maxima SYBR Green/ROX qPCR Master Mix assay (Thermo Scientific). Real-time PCR and subsequent calculations were performed by a StepOnePlus Real-Time PCR System (Applied Biosystem). Real-time PCR primer sequences are listed in Supplementary Table 3.

### Biotin-Labeled miR-200b Pulldown Assay

The biotin-labeled miR-200b or the biotin-labeled negative control (*C. elegans* miR-67) was transfected into cells for 48 h, and then whole-cell lysates were collected. Cell lysates were mixed with streptavidin-coupled Dynabeads (Invitrogen) and incubated at 4°C on a rotator overnight. After the beads were washed thoroughly, the bead-bound RNA was isolated and subjected to reverse transcription followed by real-time PCR analysis. Input RNA was extracted and served as a control.

### Whole-Embryo Culture

The whole-embryo culture system was previously described (5,6). E8.5 embryos were cultured in 4 mL rat serum at 38°C in 30 revolutions/min rotation in the roller bottle system. The culture bottles were gassed with 5% $O_2$/5% $CO_2$/90% $N_2$ for the first 24 h and 10% $O_2$/5% $CO_2$/85% $N_2$ for the last 12 h.

### TUNEL Assay

The TUNEL assay was performed by using the In Situ Cell Death Detection kit (Millipore) (5). After transfection and high glucose treatment, cells were fixed with 4% paraformaldehyde in PBS and incubated with TUNEL reagent, counterstained with DAPI, and mounted with aqueous mounting medium (Sigma). TUNEL-positive cells in each well were counted. The percentage of apoptotic cells was calculated as the number of TUNEL-positive (apoptotic) cells, divided by the total number of cells in a microscopic field from three separate experiments.

### Statistics

Data are presented as means ± SE. Three embryos from three separate dams were used for the in vivo studies, and cell culture experiments were repeated three times. One-way ANOVA was performed using SigmaStat 3.5 software, and a Tukey test was used to estimate the significance. Statistical significance was accepted when $P < 0.05$.

## RESULTS

### High Glucose In Vivo and In Vitro Induces miR-200b Overexpression Through Oxidative Stress

The levels of miR-200b were significantly increased in WT embryos exposed to maternal diabetes compared with WT embryos from nondiabetic dams (Fig. 1*A*). SOD1-overexpressing embryos had significantly lower levels of miR-200b than those in their WT littermates (Fig. 1*A*). For ascertainment of whether high glucose of maternal diabetes is the primary factor that stimulates miR-200b expression, embryos from insulin-treated dams were analyzed. Insulin treatment significantly lowered blood glucose levels in diabetic dams from 22.7 ± 1.2 mmol/L to 13.6 ± 0.6 mmol/L glucose and blunted maternal diabetes–increased miR-200b expression (Fig. 1*A*).

To reveal whether high glucose in vitro has a similar effect on miR-200b expression, neural stem cells were cultured under normal glucose (5 mmol/L glucose) or high glucose (16.6, 25, and 33.3 mmol/L glucose) conditions. High glucose increased miR-200b expression in a dose-dependent manner, and the increased miR-200b expression reached a plateau at 25 mmol/L glucose (Fig. 1*B*). The 25 mmol/L glucose level was comparable with the high blood glucose levels seen in the diabetic dams (glucose levels 22.7 ± 1.2 mmol/L). In a time course study, 25 mmol/L glucose stimulated miR-200b expression at 12, 24, 48, 72, and 96 h, with the highest increase observed at 24 h (Fig. 1*C* and Supplementary Fig. 1*A*). Treatment with the SOD1 mimetic tempol abolished high glucose–increased miR-200b expression (Fig. 1*D*) Mannitol was used as an osmotic control of glucose. High mannitol concentrations did not affect miR-200b expression (Fig. 1*E* and *F*).

### miR-200b Interacts With CITED2 mRNA

A miRNA target prediction algorithm (miRanda) revealed CITED2 as a potential target of miR-200b. There are two predicted binding sites of miR-200b in the 3′-UTR of CITED2 mRNA (Fig. 2*A*). To test whether CITED2 is a true target of miR-200b, we examined the association of miR-200b with the CITED2 mRNA by an RNA pulldown assay using biotin-labeled miR-200b. To ensure the transfection efficiency of miR-200b, we examined the levels of miR-200b and small nuclear RNA U6 (which served as the

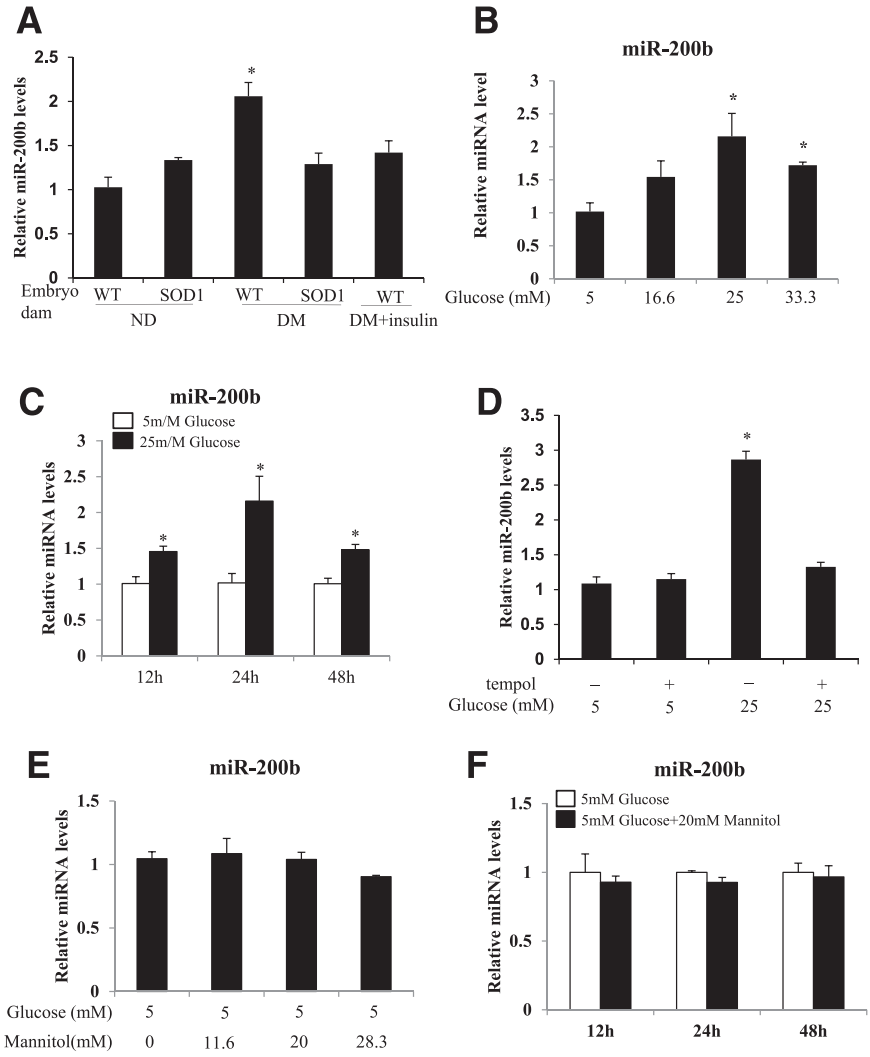


**Figure 1**—High glucose in vivo and in vitro upregulates miR-200b expression through oxidative stress. *A*: miR-200b levels were determined by real-time PCR and normalized by U6 in WT and SOD1-overexpressing embryos from nondiabetic (ND) (nondiabetic dam glucose levels: 7.1 ± 0.3 mmol/L) and diabetic (DM) dams (diabetic dam glucose levels: 22.7 ± 1.2 mmol/L) and in WT embryos from diabetic dams with insulin pellet implantation throughout the experimental course (glucose levels in diabetic dam with insulin treatment: 13.6 ± 0.6 mmol/L). Experiments were conducted using 6 embryos from 6 different dams ($n$ = 6) per group. *Significant differences ($P$ < 0.05) compared with other groups. *B*: miR-200b levels in neural stem cells cultured under normal glucose (5 mmol/L glucose) or high glucose (16.6, 25, and 33.3 mmol/L glucose) conditions for 24 h. *C*: miR-200b levels in cells cultured under 5 mmol/L or 25 mmol/L glucose conditions for 12, 24, and 48 h. *D*: miR-200b levels in cells under 5 mmol/L or 25 mmol/L glucose in the absence or presence of the SOD1 mimetic tempol (100 μmol/L) for 24 h. *E*: miR-200b levels in cells cultured under 5 mmol/L glucose conditions with or without high mannitol (11.7, 20, and 28.3 mmol/L mannitol) for 24 h. *F*: miR-200b levels in cells cultured under 5 mmol/L glucose conditions with or without 20 mmol/L mannitol for 12, 24, and 48 h. Cell culture experiments were repeated three times ($n$ = 3). *Significant differences ($P$ < 0.05) compared with other groups (*A*, *B*, and *D*) or the 5 mmol/L glucose groups (*C*).

control) after 48 h transfection. Cells transfected with the biotin-labeled miR-200b displayed elevated miR-200b levels along with no change in RNA U6 levels (Fig. 2*B*).

We examined the abundance of CITED2 mRNA in the RNA pulldown assay and found an eleven-fold greater enrichment of CITED2 mRNA in the pulldown beads of cell samples transfected with the biotin-labeled miR-200b compared with cells transfected with biotin-labeled control miRNA (Fig. 2*C*). Additionally, increasing the levels of miR-200b by biotin-labeled miR-200b transfection did not alter the total levels of CITED2 mRNA (Fig. 2*C*). Furthermore, the association of miR-200b with CITED2 mRNA was completely inhibited when unlabeled synthetic RNA sense strands (RSS1 and RSS2) against CITED2 3′-UTR (positions from 1514 to 1536 and 1846 to 1867, encompassing the two miR-200b binding sites) were added to the cell culture medium together with biotin-labeled miR-200b (Fig. 2*D*). Treatment with RSS1 and RSS2 had no effect on the levels of total CITED2 mRNA (Fig. 2*D*). These results strongly suggest that miR-200b directly interacts with the CITED2 mRNA and forms the miR-200b/CITED2 mRNA complex.

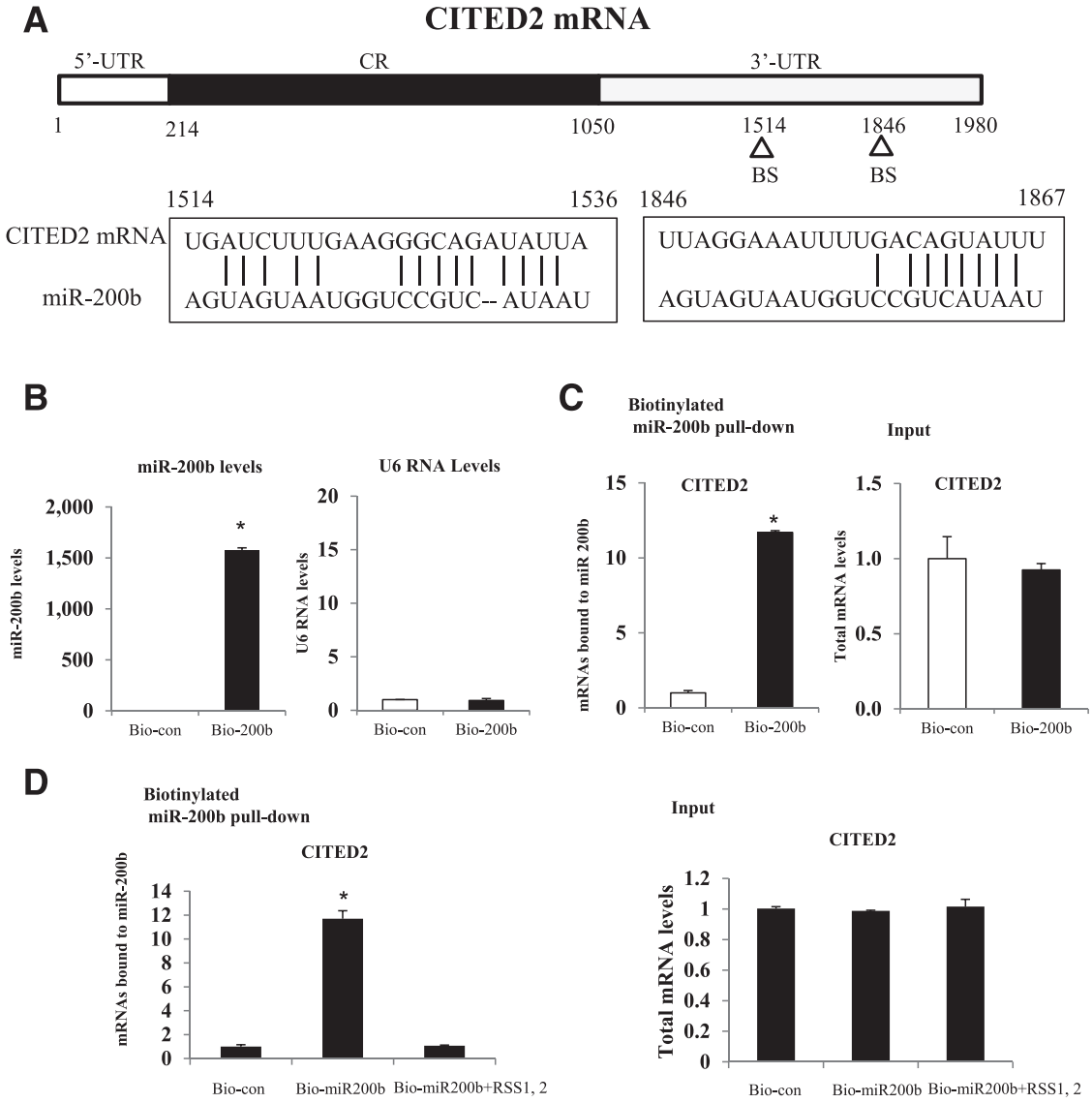


**Figure 2—** miR-200b interacts with CITED2 mRNA. *A*: Schematic representation of the CITED2 mRNA depicting the two miR-200b binding sites (BS) in its 3′-UTR. Alignment of the CITED2 mRNA sequence with miR-200b: top strand, CITED2 mRNA; bottom strand, miR-200b. *B*: miR-200b levels and U6 RNA levels after 48-h biotinylated miR-200b transfection. Bio-con, the biotin-labeled negative control; Bio-200b, biotin-labeled miR-200b. *C*: CITED2 mRNA levels in the materials pulled down by biotin–miR-200b and levels of total input CITED2 mRNA. *D*: Changes in CITED2 mRNA levels in biotin–miR-200b pulldown after addition of unlabeled synthetic RNA sense strands (RSS1 and RSS2) against CITED2 3′-UTR (positions from 1514 to 1536 and 1846 to 1867, encompassing the two miR-200b binding sites) to the reaction buffer in the RNA pulldown assay. Experiments were repeated three times ($n = 3$). *Significant differences ($P < 0.05$) compared with the control group or the other two groups.

### miR-200b Represses CITED2 Expression

For investigation of the functionality of the miR-200b/CITED2 mRNA complex, luciferase reporter constructs were used to examine whether miR-200b regulates CITED2 expression. miRNAs repress translation and/or degrade mRNA by binding to seed site sequences located within the 3′-UTR of mRNA (24). The CR, 3′-UTR, or the franking regions (F1, F2) of the miR-200b binding sites in CITED2 mRNA were subcloned into the pmirGLO dual-luciferase miRNA target expression vector to generate CR-Luc, UTR-Luc, F1-Luc, and F2-Luc reporter constructs (Fig. 3*A*). Ectopic miR-200b overexpression decreased the 3′-UTR luciferase reporter activity (Fig. 3*A*), but it failed to inhibit the CR reporter activity (Fig. 3*A*), indicating that miR-200b represses CITED2 mRNA translation through interaction with the CITED2 3′-UTR rather than with its CR. Moreover, the luciferase activities of the F1-Luc and F2-Luc constructs were significantly inhibited by the miR-200b mimic (Fig. 3*A*).

To further characterize the specific miR-200b binding sites in the CITED2 3′-UTR, deletion mutations of the miR-200b binding sites in F1 or F2 fragments of the CITED2 3′-UTR were also performed, in which the

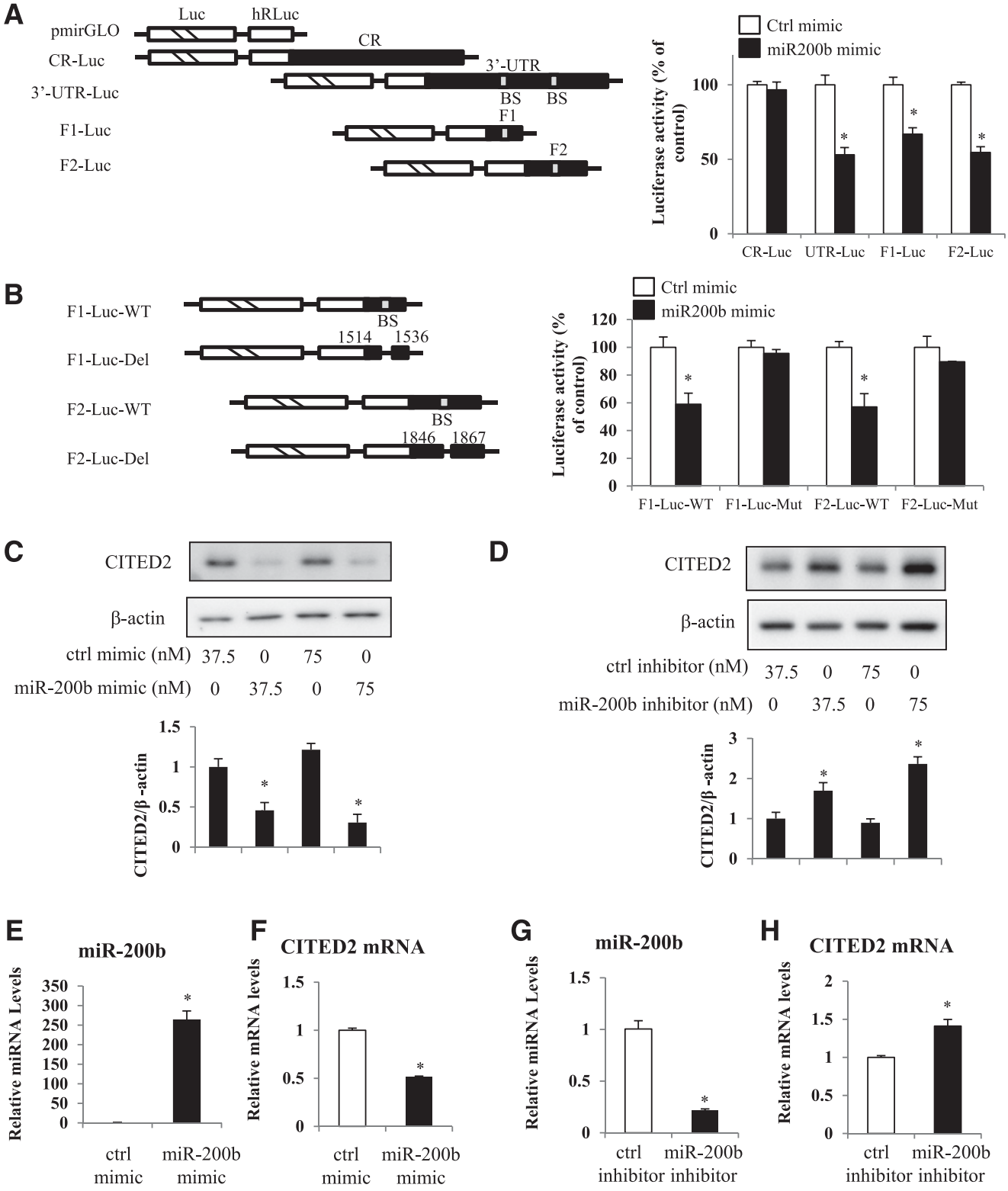


**Figure 3**—miR-200b inhibits CITED2 expression. *A*: Levels of CITED2 CR, 3′-UTR, F1, or F2 (two 3′-UTR fragments encompassing the two specific binding sites of miR-200b) luciferase reporter activities after miR-200b transfection. Right: Schematic of different chimeric firefly luciferase CITED2 reporters. BS, predicted miR-200b binding site. Left: Levels of activities of luciferase reporters containing CITED2 CR, 3′-UTR, F1, or F2. Twenty-four hours after miR-200b transfection, cells were transfected with different CITED2 luciferase reporter plasmids. Levels of firefly and Renilla luciferase activities were assayed 24 h later. Results were normalized to the Renilla luciferase activities and expressed as the means ± SE data from three separate experiments ($n$ = 3). *B*: Effect of deleting (Del) the two miR-200b binding sites in the CITED2 3′-UTR on luciferase reporter activities after miR-200b transfection. *C*: Changes in CITED2 protein expression after cells transfected with different doses of the miR-200 mimic for 48 h. *D*: Protein levels of CITED2 in cells transfected with the miR-200b inhibitor for 48 h. *E*: Levels of miR-200b in cells transfected with 75 nmol/L miR-200b

nucleotides spanning positions 1514–1536 or 1846–1867 of the CITED2 3′-UTR were eliminated (Fig. 3*B*). The mutant constructs of F1 and F2 lacking the miR-200b binding sites were refractory to the decrease in luciferase activities by miR-200b (Fig. 3*B*).

The repression of CITED2 expression by miR-200b was experimentally further validated. CITED2 protein expression was diminished by 37.5 or 75 nmol/L miR-200b mimic (Fig. 3*C*). On the other hand, CITED2 protein levels increased accordingly when cells were transfected with 37.5 or 75 nmol/L miR-200 inhibitor (Fig. 3*D*). When miR-200b levels were increased remarkably by transfection with the miR-200b mimic (Fig. 3*E*), CITED2 mRNA levels were significantly decreased (Fig. 3*F*). The miR-200b inhibitor suppressed endogenous miR-200b levels and, thus, increased CITED2 mRNA levels (Fig. 3*G* and *H*).

Altogether, these results indicate that miR-200b interacts with CITED2 mRNA via the specific binding sites located in its 3′-UTR, thus silencing CITED2 expression by degrading mRNA and blocking translation.

### High Glucose Downregulates CITED2 Expression Through miR-200b

For determination of whether high glucose affects CITED2 expression, C17.2 cells were treated with 25 mmol/L glucose for 12, 24, 48, and 72 h. High glucose downregulated CITED2 at both protein and mRNA levels (Fig. 4*A* and *B* and Supplementary Fig. 1*B*). In contrast, the glucose osmotic control, mannitol, did not affect CITED2 expression (Fig. 4*A* and *B*). Consistent with these in vitro findings, CITED2 protein and mRNA levels were significantly decreased in WT embryos exposed to maternal diabetes compared with WT embryos from nondiabetic dams (Fig. 4*C* and *D*). Under maternal diabetic conditions, SOD1-overexpressing embryos had significantly higher levels of CITED2 protein and mRNA than those in their WT littermates (Fig. 4*C* and *D*). Moreover, the SOD1 mimetic tempol abolished high glucose–induced CITED2 reduction at both protein (Fig. 4*E* and Supplementary Fig. 2) and mRNA (Fig. 4*F*) levels.

To explore whether miR-200b mediates the inhibitory effect of high glucose on CITED2 expression, cells were transfected with the miR-200b mimic or inhibitor under normal glucose (5 mmol/L) or high glucose (25 mmol/L) conditions. The miR-200b mimic as well as high glucose inhibited CITED2 expression (Fig. 4*G*). The miR-200b inhibitor abrogated high glucose–suppressed CITED2 protein expression (Fig. 4*H*).

### High Glucose Induces UPR Signaling and ER Stress Through miR-200b

Maternal diabetes induces ER stress in the developing embryos, which causes apoptosis in the neural tube leading to NTDs (5). For testing of whether miR-200b induces UPR signaling and ER stress, the phosphorylated levels of the two major UPR sensors, IRE1α and PERK, were assessed. Protein levels of phosphorylated (p)-IRE1α, p-PERK, and p-eIF2α were significantly increased by the miR-200b mimic (Fig. 5*A* and *B*). The ER stress marker CHOP was significantly higher in cells transfected with the miR-200b mimic compared with the control mimic (Fig. 5*A* and *B*). Additionally, UPR activation and ER stress markers induced by high glucose were abrogated by the miR-200b inhibitor (Fig. 5*C* and *D*). Taken together, these data indicate that miR-200b is involved in the induction of UPR and ER stress by high glucose.

### Silencing CITED2 Promotes UPR and ER Stress

Because miR-200b overexpression induces UPR and ER stress and because CITED2 is a downstream effector of miR-200b, we tested whether reduced CITED2 expression promotes UPR and ER stress. To this end, CITED2 protein and mRNA were transiently inhibited by siRNA. Treatment with 35 nmol/L CITED2 siRNA reduced CITED2 protein and mRNA levels to ~75% and 50% of those in controls, respectively (Fig. 6*A* and *B*). When CITED2 was silenced, the phosphorylation of IRE1α, PERK, and eIF2α and the expression of CHOP were upregulated (Fig. 6*C*).

### miR-200b Induces UPR and ER Stress Through Silencing CITED2

Because both increasing miR-200b and decreasing CITED2 activate UPR and ER stress, we further investigated whether both high glucose and miR-200b induce UPR and ER stress by inhibiting CITED2. Cells were cotransfected with the CITED2 plasmid and the miR-200b mimic. As expected, phosphorylation of IRE1α, PERK, eIF2α, and the ER stress marker CHOP were significantly increased, and CITED2 was decreased by the miR-200b mimic (Fig. 7*A* and *B*). The induction of UPR signaling and ER stress by the miR-200b mimic was attenuated when CITED2 expression, which was suppressed by the miR-200b mimic, was restored by the CITED2 plasmid (Fig. 7*A* and *B*).

CITED2 overexpression prevented UPR and ER stress induced by miR-200b, which mediates a pro-ER stress effect of high glucose. Next, we tested whether CITED2 inhibits high glucose–induced UPR and ER stress. Indeed, CITED2 overexpression blocked high glucose–triggered

for 24 h. *F*: Changes in CITED2 mRNA expression after miR-200b (75 nmol/L) transfection. *G*: miR-200b levels in cells transfected with the 75 nmol/L miR-200b inhibitor for 24 h. *H*: Effect of the miR-200b inhibitor (75 nmol/L) on CITED2 mRNA expression. Data were mean ± SE from three separate experiments ($n = 3$). *Significant differences ($P < 0.05$) compared with the control mimic or inhibitor groups (*A*, *B*, and *E–H*) or the same doses of control mimic or inhibitor groups (*C* and *D*). Ctrl, control; hRLuc, human-codon optimized Renilla luciferase.

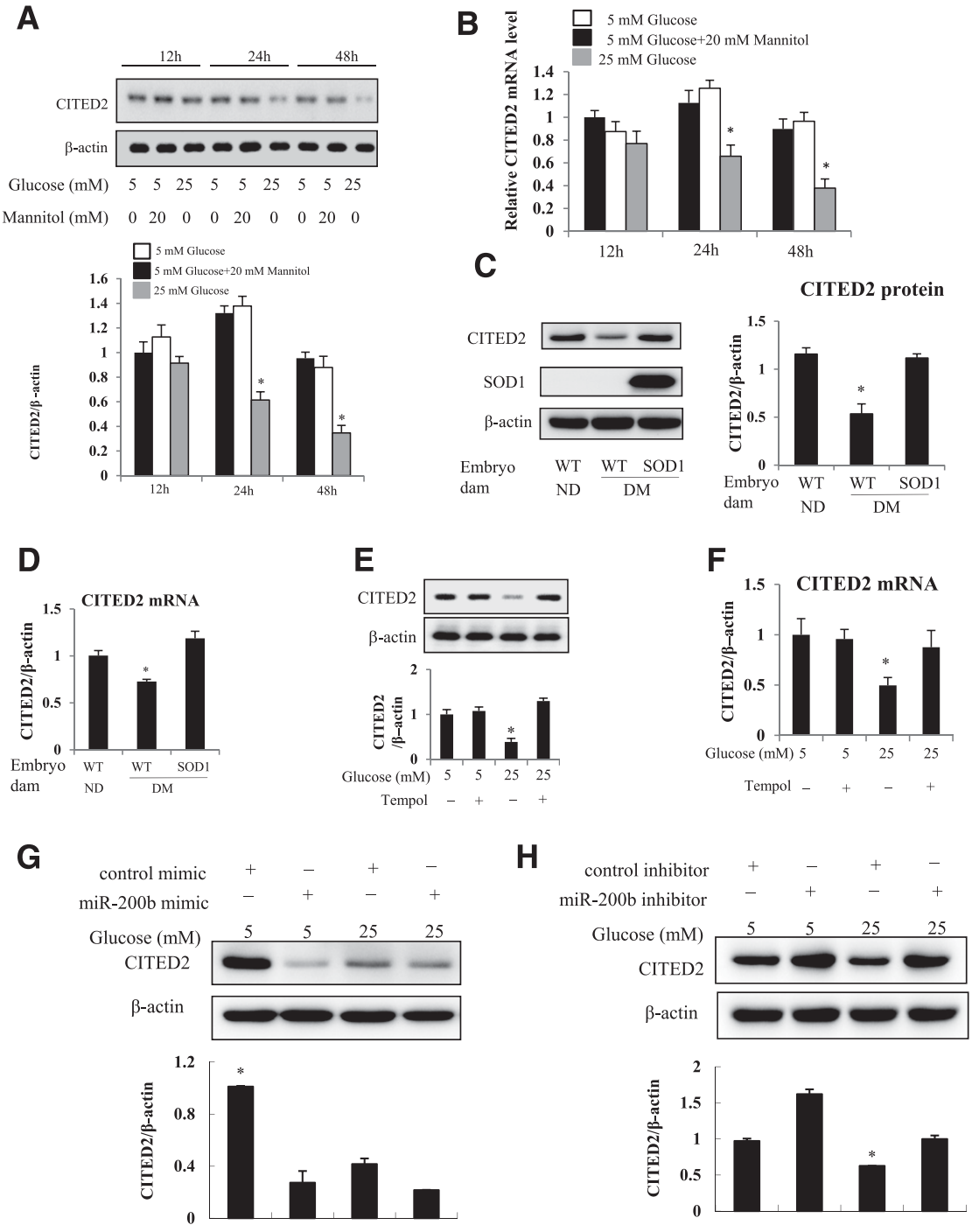


**Figure 4**—High glucose downregulates CITED2 expression through miR-200b. Changes in CITED2 protein expression (*A*) and mRNA expression (*B*) in cells cultured under 5 mmol/L glucose, 5 mmol/L glucose plus 20 mmol/L mannitol (the osmotic control of glucose), or 25 mmol/L glucose conditions for 12, 24, and 48 h. Experiments were repeated three times ($n = 3$), and the quantification of data is shown in the bar graphs. *Significant differences ($P < 0.05$) compared with the 5 mmol/L glucose group and the 5 mmol/L glucose plus 20 mmol/L mannitol group. Levels of CITED2 protein (*C*) and mRNA (*D*) in WT embryos from nondiabetic (ND) dams and WT and SOD1-overexpressing embryos from diabetic (DM) dams mated with SOD1-Tg males. Experiments were repeated three times using embryos from three different dams ($n = 3$) per group, and the quantification of the data is shown in the bar graphs. CITED2 protein levels (*E*) and mRNA levels (*F*) in cells cultured under 5 mmol/L glucose or 25 mmol/L glucose conditions in the absence or presence of tempol (100 μmol/L). The quantification of data is shown in the bar graphs. *G*: Levels of CITED2 protein in cells transfected with the control oligo or the miR-200b mimic under 5 mmol/L or 25 mmol/L glucose conditions. *H*: Levels of CITED2 protein expression in cells transfected with the control oligo or the miR-200b inhibitor under 5 mmol/L or 25 mmol/L glucose conditions. In *E–H*, experiments were repeated three times ($n = 3$). *Significant differences ($P < 0.05$) compared with the other three groups.

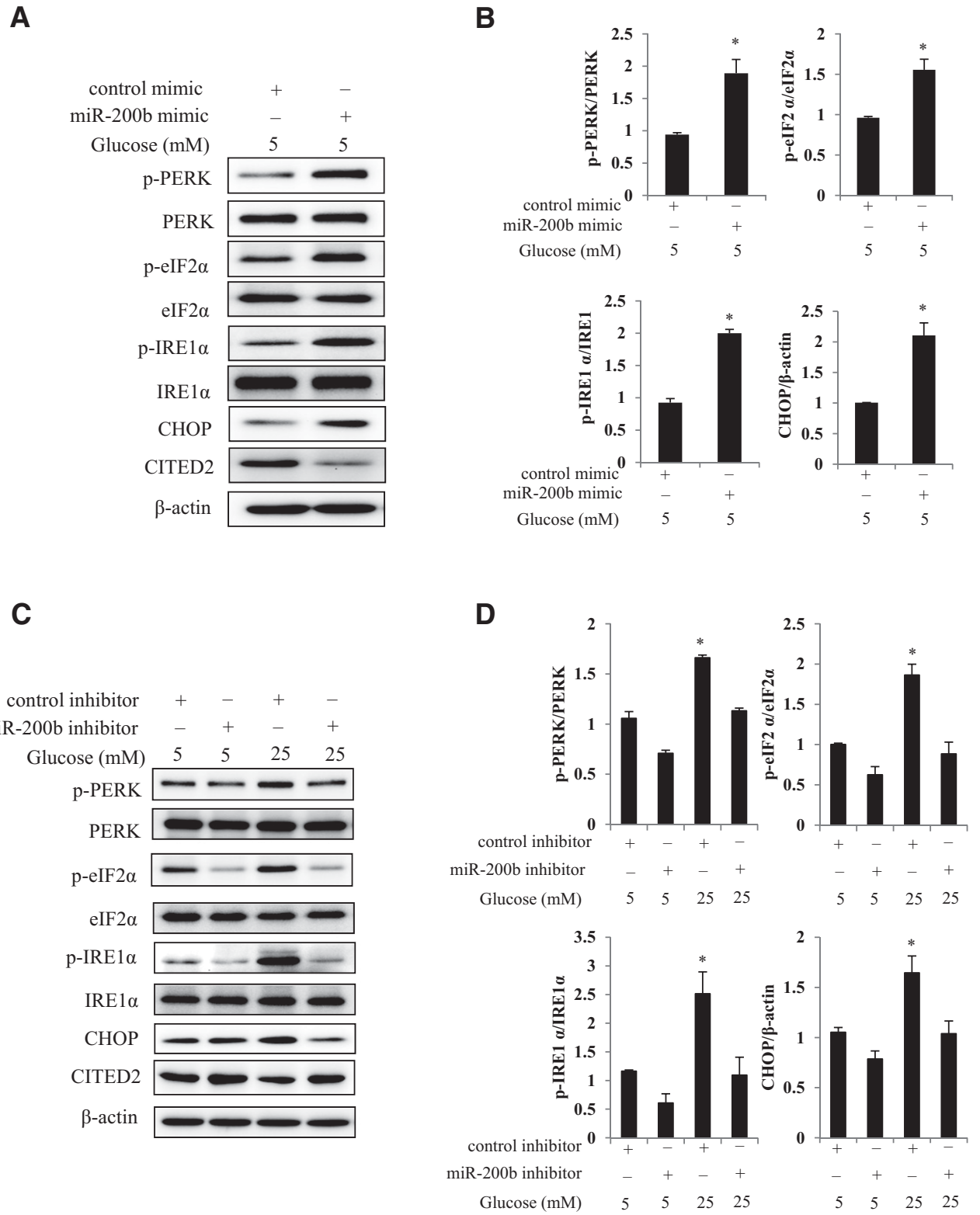


**Figure 5—**High glucose induces UPR and ER stress through miR-200b. Protein levels of p-PERK, PERK, p-eIF2α, eIF2α, p-IRE1α, IRE1α, CHOP, CITED2, and β-actin in cells transfected with the control oligo or the miR-200b mimic under 5 mmol/L glucose conditions (*A* and *B*) and in cells transfected with the control oligo or the miR-200b inhibitor under 5 mmol/L or 25 mmol/L glucose conditions (*C* and *D*). Experiments were repeated three times ($n = 3$), and the quantification of the data is shown in the bar graphs. *Significant differences ($P < 0.05$) compared with the other group or groups.

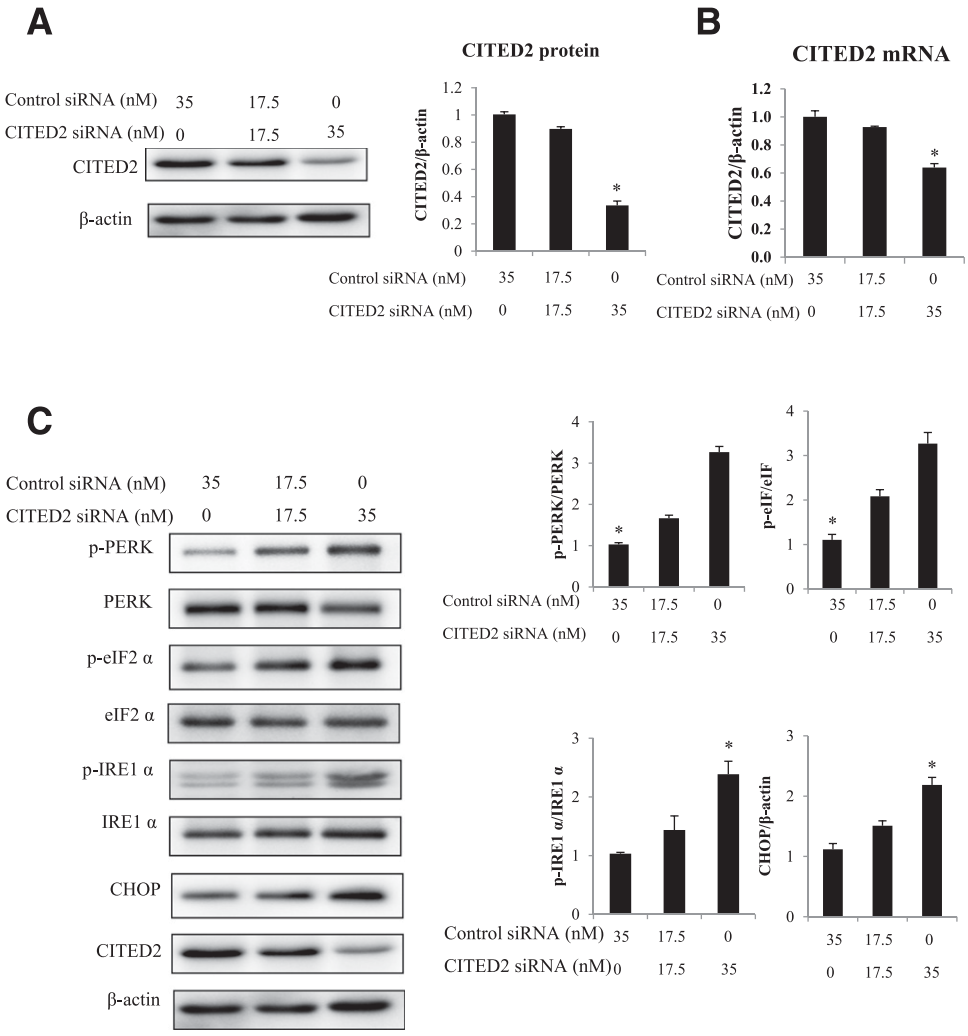


**Figure 6**—CITED2 silencing promotes UPR and ER stress. CITED2 protein (*A*) and mRNA levels (*B*) in cells transfected with different concentrations of the control siRNA and the CITED2 siRNA. *C*: Changes in p-PERK, PERK, p-eIF2α, eIF2α, p-IRE1α, IRE1α, and CHOP protein expression in cells transfected with the CITED2 siRNA. Experiments were repeated three times ($n = 3$), and the quantification of data is shown in the bar graphs. *Significant differences ($P < 0.05$) compared with the other groups.

phosphorylation of IRE1α, PERK, eIF2α, and CHOP upregulation (Fig. 7*C* and *D*).

### CITED2 Downregulation by miR-200b Mediates High Glucose–Induced ER Stress-Dependent Apoptosis

To define the biological consequence of high glucose–induced miR-200b upregulation and consequent CITED2 downregulation, we assessed the number of apoptotic cells and caspase cleavage. When cells were exposed to high glucose, apoptotic cells were robustly present, whereas the miR-200b inhibitor protected cells from undergoing high glucose–induced apoptosis (Fig. 8*A* and *B*). Likewise, CITED2 overexpression significantly reduced high glucose–increased TUNEL-positive cell numbers (Fig. 8*C* and *D*). Moreover, the ER stress inhibitor 4-phenylbutyric acid (4-PBA) blocked CITED2 knockdown-induced apoptosis (Fig. 8*E* and *F*). High glucose increased the abundance of cleaved caspase 3, and both the miR-200b inhibitor and CITED2 overexpression blocked high glucose–induced caspase cleavage (Fig. 8*G* and *H*). 4-PBA treatment prevented CITED2 knockdown–induced caspase 3 cleavage (Fig. 8*I*).

We previously found that the ER stress inhibitor, 4-PBA, blocked high glucose–induced apoptosis (5). Together with our previous findings, our data suggest that the miR-200b–CITED2 circuit mediates the proapoptotic effect of high glucose by activating UPR and ER stress.

### miR-200b Inhibitor Reverses High Glucose–Induced CITED2 Downregulation, ER Stress, and NTDs in Cultured Embryos

To test whether the miR-200b inhibitor has any effect on high glucose–induced NTDs, we used the ex vivo whole-embryo culture system as previously described (5). As observed in cultured cells (Fig. 3*G*), the miR-200b inhibitor suppressed endogenous miR-200b

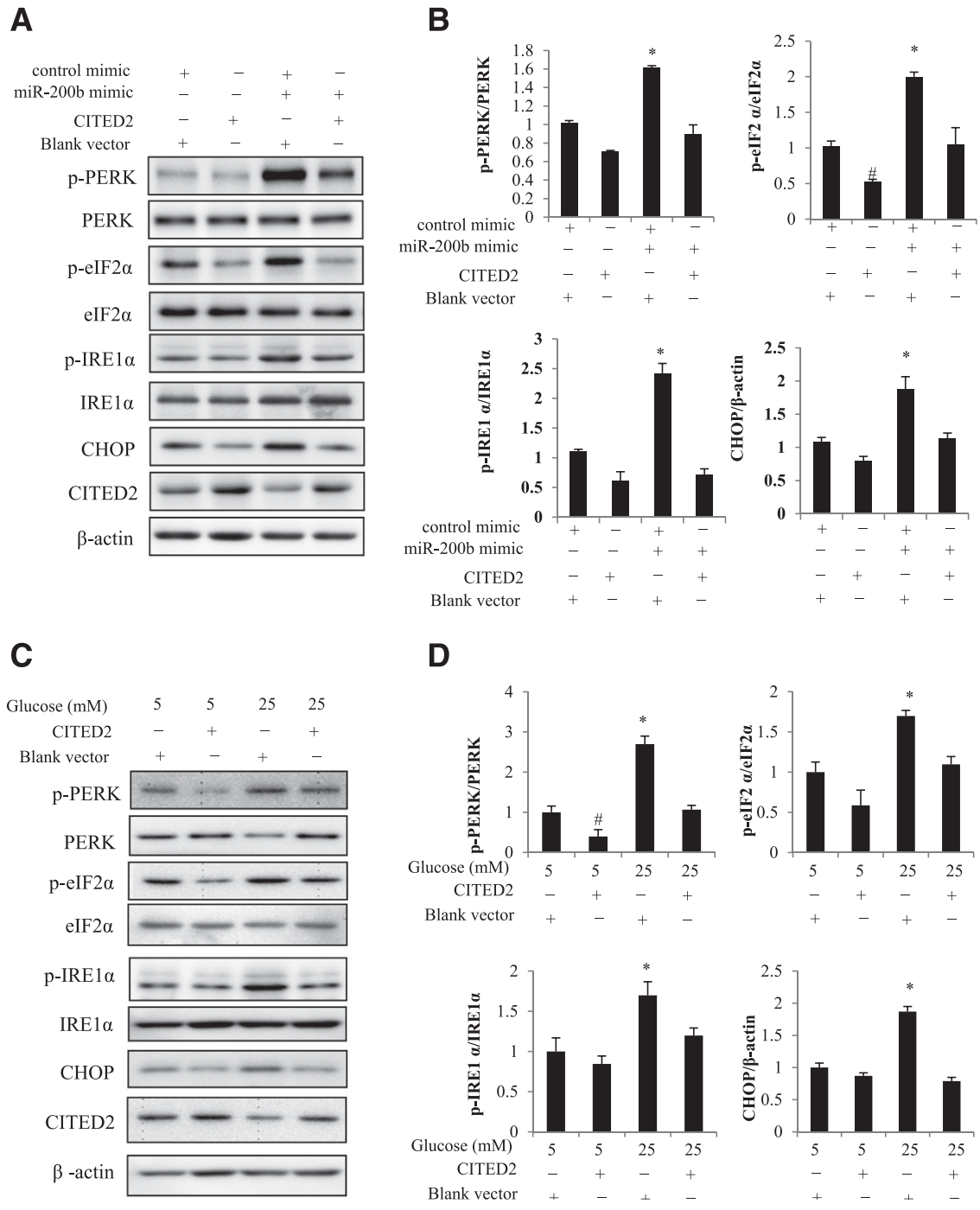


**Figure 7—**Restoring CITED2 expression blocks miR-200b– or high glucose–induced ER stress. *A* and *B*: Protein levels of ER stress markers p-PERK, PERK, p-eIF2α, eIF2α, p-IRE1α, IRE1α, and CHOP in cells transfected with the CITED2 plasmid and cotransfected with the control oligo or the miR-200b mimic. *C* and *D*: Protein levels of ER stress markers p-PERK, PERK, p-eIF2α, eIF2α, p-IRE1α, IRE1α, and CHOP in cells transfected with the blank vector or the CITED2 plasmid and then treated with 5 mmol/L glucose or 25 mmol/L glucose. Experiments were repeated three times ($n = 3$), and the quantification of data is shown in the bar graphs. * and # indicate significant differences ($P < 0.05$) compared with the other three groups.

expression in cultured embryos (Fig. 8*J*) and suppressed high glucose–induced miR-200b upregulation (Fig. 8*J*). Consistent with the blockade of high glucose–induced miR-200b expression, the miR-200b inhibitor reversed the downregulation of CITED2 mRNA and protein expression (Fig. 8*K* and *L*). Furthermore, the miR-200b inhibitor suppressed high glucose–induced ER stress by decreasing ER stress markers, immunoglobulin heavy-chain-binding protein (BiP), and CHOP (Fig. 8*K* and *L*), leading to amelioration of NTDs (Fig. 8*M*).

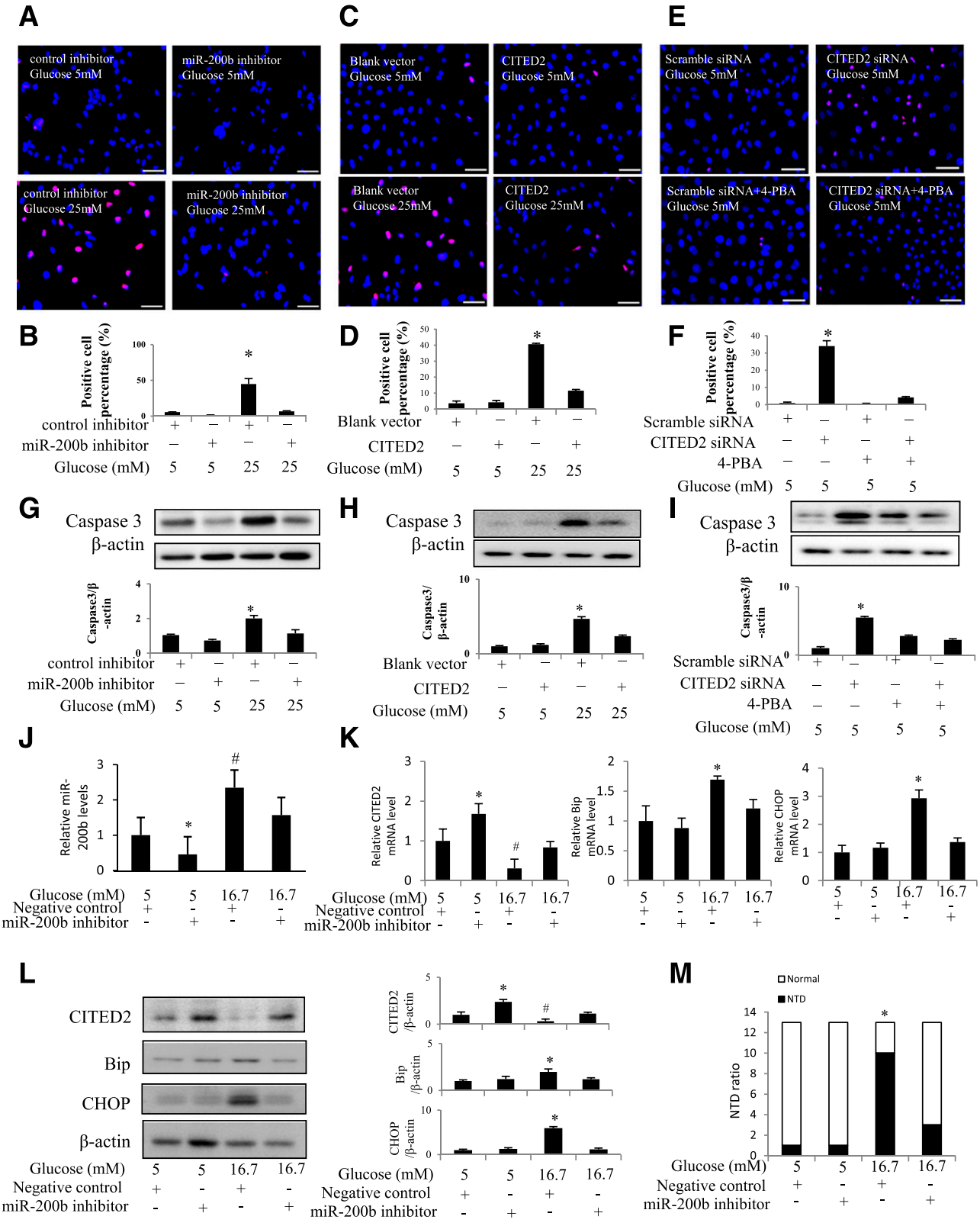


**Figure 8—**The miR-200b–CITED2 circuit mediates the proapoptotic effect of high glucose through ER stress. Representative images of the TUNEL assay and quantitative data of apoptotic cell numbers in cells transfected with the control oligo or the miR-200b inhibitor under 5 mmol/L glucose or 25 mmol/L glucose conditions (*A* and *B*), in cells transfected with the blank vector or the CITED2 plasmid under 5 mmol/L glucose or 25 mmol/L glucose conditions (*C* and *D*), and in cells transfected with scramble siRNA or CITED2 siRNA in the absence or presence of 2 mmol/L 4-PBA (*E* and *F*). Apoptotic cells were labeled red, and all cell nuclei were stained by DAPI (blue). Experiments were repeated three times ($n = 3$). Protein levels of cleaved caspase 3 in cells under 5 mmol/L or 25 mmol/L glucose conditions with or without the miR-200b inhibitor (*G*), in cells under 5 mmol/L or 25 mmol/L glucose conditions with or without the transfection of the CITED2 plasmid

## DISCUSSION

Hydrogen peroxide, one of the biological reactive oxygen species, increases miR-200b expression (34). High glucose enhances reactive oxygen species production and simultaneously impairs endogenous antioxidant capacity, leading to oxidative stress (35–38). Overexpression of SOD1, an antioxidant enzyme, in SOD1-Tg mice blocks maternal diabetes–induced oxidative stress (39–41). We found that SOD1 abrogated miR-200b upregulation induced by maternal diabetes. Furthermore, we showed that high glucose–increased miR-200b was blunted in cells treated with the SOD1 mimetic, tempol. Consistent with a prior report (34), our findings support the hypothesis that oxidative stress mediates the stimulative effect of high glucose on miR-200b expression.

The current study revealed CITED2 as a new target of miR-200b. The miR-200b mimic suppressed CITED2 expression, whereas a miR-200b inhibitor reversed high glucose–repressed CITED2 expression. Biotin-labeled miR-200b directly binds to CITED2 mRNA. We identified two miR-200b binding sites in the CITED2 3′-UTR. Previous global gene expression studies using DNA microarray (10) could not reveal miRNA expression. For protein coding genes, consistent with our finding, a gene profiling study in neurulation stage embryos (10) revealed that maternal diabetes suppressed CITED2 expression. Our study further uncovers the mechanism underlying CITED2 downregulation that is due to miR-200b upregulation. CITED2 deletion causes excessive apoptosis in the developing neuroepithelium leading to NTDs (29,42). Consistent with the findings in the CITED2 knockout mouse model (29,42), we have found that silencing CITED2 triggers apoptosis. The findings in our study support a possible mechanism for CITED2 deficiency–induced apoptosis: CITED2 deficiency seems to promote ER stress, which causes apoptosis. This is in agreement with our previous findings that ER stress mediates the proapoptotic effects of high glucose (5). Thus, during normal development, CITED2 may protect the embryos against ER stress caused by environmental perturbations or stress conditions. Our ex vivo experiments demonstrated that miR-200b inhibition reversed high glucose–repressed CITED2 and, thereby, ameliorated ER stress and NTDs in the developing embryo. Although these ex vivo findings support the critical involvement of the miR-200b–CITED2–ER stress pathway in high glucose–induced NTDs, one shortcoming of our study is lack of in vivo tests of this proposed pathway in diabetes-induced NTDs.

An intriguing question is whether miRNA dysregulation can directly cause disruption of ER homeostasis. Indeed, the results in the current study support this hypothesis that miRNA dysregulation causes UPR activation and ER stress. Increased miR-200b and decreased CITED2 act upstream of ER imbalance and UPR activation because both ectopic miR-200b overexpression and CITED2 silencing activate UPR leading to ER stress. However, it is still unclear how the miR-200b–CITED2 circuit causes UPR and ER stress. One possibility is that CITED2 is required for gene expression essential for ER homeostasis. CITED2 interacts with a group of transcription factors and transcription coactivators including PGC-1α (43). CITED2 enhances PGC-1α activity (44), which resolves ER homeostatic imbalance through activating transcription factor 6 (45).

The C17.2 cells resemble cells in the developing neuroepithelium in responding to high glucose in inducing ER stress and apoptosis (46,47). Our experiments that were conducted in C17.2 cells are in vitro in nature, and the 17.2 cell line is currently among the best in vitro model in research of diabetes-induced NTDs. Although factors in early embryonic development may contribute to late NTD formation, the key period for mouse neurulation is from E8.0 to E10 (total 48 h) (3). Nevertheless, high glucose mimics maternal diabetes to increase miR-200b expression and decrease CITED2 expression in C17.2 cells even after 72 h and 96 h. Thus, these evidences collectively support the C17.2 cell line as a suitable model in our studies.

We recently discovered the apoptosis signal-regulating kinase 1 (ASK1)–forkhead transcription factor 3a (FoxO3a)–caspase 8 pathway as the major teratogenic pathway (3). FoxO3a functions as a pleiotropic regulator of apoptosis. FoxO3a downregulation decreases miRNA expression in cancer cells (48), suggesting that FoxO3a stimulates miRNA expression. Future studies may reveal whether FoxO3a mediates the stimulatory effect of maternal diabetes on miR-200b expression. The miR-200b–CITED2 pathway induces ER stress, which causes caspase 8 activation (46,49). Therefore, the ASK1–FoxO3a–caspase 8 pathway and the miR-200b–CITED2 pathway may converge on caspase 8 activation.

In summary, we have found that hyperglycemia-induced oxidative stress increases miR-200b expression leading to CITED2 repression. The miR-200b–CITED2 circuit promotes UPR and ER stress and, thus, mediates the proapoptotic effect of high glucose. We, therefore, have revealed a new link between high glucose–induced ER

(*H*), and in cells treated with CITED2 siRNA with or without 4-PBA (*I*). Levels of miR-200b (*J*), CITED2, BiP, and CHOP mRNA and proteins (*K* and *L*) in embryos cultured under 5 mmol/L glucose or 16.7 mmol/L glucose (high glucose) with or without the miR-200b inhibitor are shown. E8.5 embryos were cultured for 36 h, and the number of NTD and normally developed (Normal) embryos are shown (*M*). $\chi^2$ test was used for statistical analyses (*M*). Experiments were repeated three times ($n = 3$), and the quantification of data is shown in the bar graph. * and # indicate significant differences ($P < 0.05$) compared with the other three groups.

stress and the miR-200b–CITED2 circuit, which may play an important role in diabetic embryopathy.

**Acknowledgments.** The authors are grateful for the support from the Office of Dietary Supplements, National Institutes of Health. The authors thank Dr. Julie Wu at the University of Maryland School of Medicine for critical reading and editing assistance.

**Funding.** This study was supported by National Institutes of Health R01-DK-083243, R01-DK-101972, R56-DK-095380, and R01-DK-103024 and the American Diabetes Association Basic Science Award (1-13-BS-220).

**Duality of Interest.** No potential conflicts of interest relevant to this article were reported.

**Author Contributions.** H.G., J.Y., and D.D. researched data. Q.Z., J.-Y.W., and S.F. participated in data analyses and experimental design. P.Y. conceived the project, designed the experiments, and wrote the manuscript. All authors approved the final version of the manuscript. P.Y. is the guarantor of this work and, as such, had full access to all the data in the study and takes responsibility for the integrity of the data and the accuracy of the data analysis.

## References

1. Allen DA, Yaqoob MM, Harwood SM. Mechanisms of high glucose-induced apoptosis and its relationship to diabetic complications. J Nutr Biochem 2005;16:705–713
2. Susztak K, Raff AC, Schiffer M, Böttinger EP. Glucose-induced reactive oxygen species cause apoptosis of podocytes and podocyte depletion at the onset of diabetic nephropathy. Diabetes 2006;55:225–233
3. Yang P, Li X, Xu C, et al. Maternal hyperglycemia activates an ASK1-FoxO3a-caspase 8 pathway that leads to embryonic neural tube defects. Sci Signal 2013;6:ra74
4. Li X, Weng H, Xu C, Reece EA, Yang P. Oxidative stress-induced JNK1/2 activation triggers proapoptotic signaling and apoptosis that leads to diabetic embryopathy. Diabetes 2012;61:2084–2092
5. Li X, Xu C, Yang P. c-Jun NH2-terminal kinase 1/2 and endoplasmic reticulum stress as interdependent and reciprocal causation in diabetic embryopathy. Diabetes 2013;62:599–608
6. Yang P, Zhao Z, Reece EA. Involvement of c-Jun N-terminal kinases activation in diabetic embryopathy. Biochem Biophys Res Commun 2007;357:749–754
7. Yang P, Zhao Z, Reece EA. Activation of oxidative stress signaling that is implicated in apoptosis with a mouse model of diabetic embryopathy. Am J Obstet Gynecol 2008;198:130.e131–e137
8. Greene MF, Hare JW, Cloherty JP, Benacerraf BR, Soeldner JS. First-trimester hemoglobin A1 and risk for major malformation and spontaneous abortion in diabetic pregnancy. Teratology 1989;39:225–231
9. Miller E, Hare JW, Cloherty JP, et al. Elevated maternal hemoglobin A1c in early pregnancy and major congenital anomalies in infants of diabetic mothers. N Engl J Med 1981;304:1331–1334
10. Salbaum JM, Kappen C. Neural tube defect genes and maternal diabetes during pregnancy. Birth Defects Res A Clin Mol Teratol 2010;88:601–611
11. Phelan SA, Ito M, Loeken MR. Neural tube defects in embryos of diabetic mice: role of the Pax-3 gene and apoptosis. Diabetes 1997;46:1189–1197
12. Pavlinkova G, Salbaum JM, Kappen C. Maternal diabetes alters transcriptional programs in the developing embryo. BMC Genomics 2009;10:274
13. Wentzel P, Gäreskog M, Eriksson UJ. Decreased cardiac glutathione peroxidase levels and enhanced mandibular apoptosis in malformed embryos of diabetic rats. Diabetes 2008;57:3344–3352
14. Gareskog M, Cederberg J, Eriksson UJ, Wentzel P. Maternal diabetes in vivo and high glucose concentration in vitro increases apoptosis in rat embryos. Reprod Toxicol 2007;23:63–74
15. Fine EL, Horal M, Chang TI, Fortin G, Loeken MR. Evidence that elevated glucose causes altered gene expression, apoptosis, and neural tube defects in a mouse model of diabetic pregnancy. Diabetes 1999;48:2454–2462
16. Bartel DP. MicroRNAs: target recognition and regulatory functions. Cell 2009;136:215–233
17. Xiao L, Cui YH, Rao JN, et al. Regulation of cyclin-dependent kinase 4 translation through CUG-binding protein 1 and microRNA-222 by polyamines. Mol Biol Cell 2011;22:3055–3069
18. Zhuang R, Rao JN, Zou T, et al. miR-195 competes with HuR to modulate stim1 mRNA stability and regulate cell migration. Nucleic Acids Res 2013;41:7905–7919
19. Lee RC, Feinbaum RL, Ambros V. The C. elegans heterochronic gene lin-4 encodes small RNAs with antisense complementarity to lin-14. Cell 1993;75:843–854
20. Lee Y, Ahn C, Han J, et al. The nuclear RNase III Drosha initiates microRNA processing. Nature 2003;425:415–419
21. Cui YH, Xiao L, Rao JN, et al. miR-503 represses CUG-binding protein 1 translation by recruiting CUGBP1 mRNA to processing bodies. Mol Biol Cell 2012;23:151–162
22. Mukhopadhyay P, Brock G, Appana S, Webb C, Greene RM, Pisano MM. MicroRNA gene expression signatures in the developing neural tube. Birth Defects Res A Clin Mol Teratol 2011;91:744–762
23. Gu H, Li H, Zhang L, et al. Diagnostic role of microRNA expression profile in the serum of pregnant women with fetuses with neural tube defects. J Neurochem 2012;122:641–649
24. Ron D, Walter P. Signal integration in the endoplasmic reticulum unfolded protein response. Nat Rev Mol Cell Biol 2007;8:519–529
25. Ozcan U, Yilmaz E, Ozcan L, et al. Chemical chaperones reduce ER stress and restore glucose homeostasis in a mouse model of type 2 diabetes. Science 2006;313:1137–1140
26. Ozcan U, Cao Q, Yilmaz E, et al. Endoplasmic reticulum stress links obesity, insulin action, and type 2 diabetes. Science 2004;306:457–461
27. Shore GC, Papa FR, Oakes SA. Signaling cell death from the endoplasmic reticulum stress response. Curr Opin Cell Biol 2011;23:143–149
28. Groenendyk J, Peng Z, Dudek E, et al. Interplay between the oxidoreductase PDIA6 and microRNA-322 controls the response to disrupted endoplasmic reticulum calcium homeostasis. Sci Signal 2014;7:ra54
29. Bamforth SD, Bragança J, Eloranta JJ, et al. Cardiac malformations, adrenal agenesis, neural crest defects and exencephaly in mice lacking Cited2, a new Tfap2 co-activator. Nat Genet 2001;29:469–474
30. Barbera JP, Rodriguez TA, Greene ND, et al. Folic acid prevents exencephaly in Cited2 deficient mice. Hum Mol Genet 2002;11:283–293
31. Schein P, Kahn R, Gorden P, Wells S, Devita VT. Streptozotocin for malignant insulinomas and carcinoid tumor. Report of eight cases and review of the literature. Arch Intern Med 1973;132:555–561
32. Snyder EY, Deitcher DL, Walsh C, Arnold-Aldea S, Hartwieg EA, Cepko CL. Multipotent neural cell lines can engraft and participate in development of mouse cerebellum. Cell 1992;68:33–51
33. Yang P, Kriatchko A, Roy SK. Expression of ER-alpha and ER-beta in the hamster ovary: differential regulation by gonadotropins and ovarian steroid hormones. Endocrinology 2002;143:2385–2398
34. Magenta A, Cencioni C, Fasanaro P, et al. miR-200c is upregulated by oxidative stress and induces endothelial cell apoptosis and senescence via ZEB1 inhibition. Cell Death Differ 2011;18:1628–1639
35. Yang X, Borg LA, Eriksson UJ. Altered metabolism and superoxide generation in neural tissue of rat embryos exposed to high glucose. Am J Physiol 1997;272:E173–E180
36. Sakamaki H, Akazawa S, Ishibashi M, et al. Significance of glutathione-dependent antioxidant system in diabetes-induced embryonic malformations. Diabetes 1999;48:1138–1144
37. Yang P, Cao Y, Li H. Hyperglycemia induces inducible nitric oxide synthase gene expression and consequent nitrosative stress via c-Jun N-terminal kinase activation. Am J Obstet Gynecol 2010;203:185.e5–e111

38. Yang P, Li H. Epigallocatechin-3-gallate ameliorates hyperglycemia-induced embryonic vasculopathy and malformation by inhibition of Foxo3a activation. Am J Obstet Gynecol 2010;203:75.e71–e76
39. Wang F, Reece EA, Yang P. Superoxide dismutase 1 overexpression in mice abolishes maternal diabetes-induced endoplasmic reticulum stress in diabetic embryopathy. Am J Obstet Gynecol 2013;209:345.e341–e347
40. Weng H, Li X, Reece EA, Yang P: SOD1 suppresses maternal hyperglycemia-increased iNOS expression and consequent nitrosative stress in diabetic embryopathy. Am J Obstet Gynecol 2012;206:448.e441–e447
41. Li X, Weng H, Reece EA, Yang P. SOD1 overexpression in vivo blocks hyperglycemia-induced specific PKC isoforms: substrate activation and consequent lipid peroxidation in diabetic embryopathy. Am J Obstet Gynecol 2011;205:84.e81–e86
42. Yin Z, Haynie J, Yang X, et al. The essential role of Cited2, a negative regulator for HIF-1alpha, in heart development and neurulation. Proc Natl Acad Sci U S A 2002;99:10488–10493
43. Li Q, Hakimi P, Liu X, et al. Cited2, a transcriptional modulator protein, regulates metabolism in murine embryonic stem cells. J Biol Chem 2014;289:251–263
44. Sakai M, Matsumoto M, Tujimura T, et al. CITED2 links hormonal signaling to PGC-1$\alpha$ acetylation in the regulation of gluconeogenesis. Nat Med 2012;18:612–617
45. Wu J, Ruas JL, Estall JL, et al. The unfolded protein response mediates adaptation to exercise in skeletal muscle through a PGC-1$\alpha$/ATF6$\alpha$ complex. Cell Metab 2011;13:160–169
46. Wang F, Wu Y, Gu H, et al. Ask1 gene deletion blocks maternal diabetes-induced endoplasmic reticulum stress in the developing embryo by disrupting the unfolded protein response signalosome. Diabetes 2015;64:973–988
47. Gu H, Yu J, Dong D, Zhou Q, Wang JY, Yang P. The miR-322-TRAF3 circuit mediates the pro-apoptotic effect of high glucose on neural stem cells. Toxicol Sci 2015;144:186–196
48. Liu X, Feng J, Tang L, Liao L, Xu Q, Zhu S. The regulation and function of miR-21-FOXO3a-miR-34b/c signaling in breast cancer. Int J Mol Sci 2015;16:3148–3162
49. Wu Y, Wang F, Fu M, Wang C, Quon MJ, Yang P. Cellular stress, excessive apoptosis, and the effect of metformin in a mouse model of type 2 diabetic embryopathy. Diabetes 2015;64:2526–2536